

# Climbing over the potential barrier during inflation via null energy condition violation

Shi Pan<sup>1,5,6\*</sup>, Yong Cai<sup>2†</sup>, and Yun-Song Piao<sup>1,3,4,5‡</sup>

<sup>1</sup> *School of Fundamental Physics and Mathematical Sciences,  
Hangzhou Institute for Advanced Study, UCAS, Hangzhou 310024, China*

<sup>2</sup> *Institute for Astrophysics, School of Physics,  
Zhengzhou University, Zhengzhou, Henan 450001, China*

<sup>3</sup> *School of Physics, University of Chinese Academy of Sciences, Beijing 100049, China*

<sup>4</sup> *International Center for Theoretical Physics Asia-Pacific, Beijing/Hangzhou, China*

<sup>5</sup> *Institute of Theoretical Physics, Chinese Academy of Sciences,  
P.O. Box 2735, Beijing 100190, China and*

<sup>6</sup> *University of Chinese Academy of Sciences, Beijing 100190, China*

## Abstract

The violation of the null energy condition (NEC) may play a crucial role in enabling a scalar field to climb over high potential barriers, potentially significant in the very early universe. We propose a single-field model where the universe sequentially undergoes a first stage of slow-roll inflation, NEC violation, and a second stage of slow-roll inflation. Through the NEC violation, the scalar field climbs over high potential barriers, leaving unique characteristics on the primordial gravitational wave power spectrum, including a blue-tilted nature in the middle-frequency range and diminishing oscillation amplitudes at higher frequencies. Additionally, the power spectrum exhibits nearly scale-invariant behavior on both large and small scales.

PACS numbers: 98.80.-k, 98.80.Cq, 04.50.Kd

---

\* [panshi22@mails.ucas.ac.cn](mailto:panshi22@mails.ucas.ac.cn) (Corresponding author)

† [caiyong@zzu.edu.cn](mailto:caiyong@zzu.edu.cn) (Corresponding author)

‡ [yspiao@ucas.ac.cn](mailto:yspiao@ucas.ac.cn) (Corresponding author)

## I. INTRODUCTION

The detection of gravitational waves (GWs) originating from binary pulsar systems [1] and binary black hole mergers [2] has opened a new avenue for exploring gravity and the universe. Recently, several collaborations within the pulsar timing array (PTA) community, including NANOGrav [3–5], EPTA [6], PPTA [7] and CPTA [8], have announced compelling evidence of a signal consistent with stochastic GW background at the frequency  $f \simeq 1 \text{ yr}^{-1}$ .

Inflation, as the most popular paradigm of the early universe, predicts the existence of a primordial GW background [9–11] across a wide frequency range ( $10^{-18} - 10^{10} \text{ Hz}$ ), yet to be confirmed by observations [12–15]. It is interesting to ask whether the signals recently observed by PTA could originate from primordial GWs, see, e.g., [16–21] (see also [22–37]). The standard slow-roll inflation predicts a nearly scale-invariant power spectrum of primordial GWs, rigorously constrained by Planck’s data, which yields a tensor-to-scalar ratio  $r_{0.002} < 0.035$  within the observational window of the cosmic microwave background (CMB) [38]. However, PTA data indicates a highly blue-tilted GW power spectrum in the nanohertz frequency band, with a spectral index of  $n_T = 1.8 \pm 0.3$  [4, 16].

Attributing the observed signal in the PTA band to primordial GWs necessitates physics beyond standard slow-roll inflation, see, e.g., [17–19, 39–43], for recent studies. There have been numerous studies exploring the generation of a blue-tilted GW spectrum by introducing new physics beyond conventional slow-roll inflation, e.g., [40, 44–65]. An intriguing direction is to introduce a violation of the null energy condition (NEC) during inflation.

Realizing a stable NEC violation is a challenge due to the presence of ghost or gradient instabilities in the primordial perturbations associated with the NEC violation [66–73]. It is first explicitly demonstrated in the framework of effective field theory that a fully stable<sup>1</sup> NEC violation can be realized in “beyond Horndeski” theories [74–78], see also [79–94] for later developments. On this basis, it has been demonstrated that NEC violation during inflation can have significant observable effects, including: 1) an enhanced and blue-tilted power spectrum of primordial GWs with distinct features [95, 96], which could be detected by PTA [19], Advanced LIGO and Advanced Virgo [97], and Taiji [98], 2) the generation of primordial black holes and scalar-induced GWs [99], 3) an amplified parity-violation effect

---

<sup>1</sup> “Fully stable” implies that both ghost and gradient instabilities are eliminated throughout the entire history of the universe.

in primordial GWs [100, 101].

In this paper, we investigate a new model where NEC violation occurs during slow-roll inflation, enabling the inflaton to climb over a high potential barrier before transitioning back to slow-roll inflation. Unlike the model in [95], in this model, the two stages of inflation before and after NEC violation have similar energy scales. We will investigate the observable effects of NEC violation in this model on the primordial GW background through analytical and numerical calculations.

## II. THE MODEL

In our single scalar field model, the universe originates from a slow-roll inflation. As the inflaton rolls slowly down the potential, it encounters a high potential barrier (see Fig. 2 for a sketch of the potential). Typically, a slowly rolling inflaton cannot climb over this high barrier. However, through the mechanism of NEC violation, the inflaton naturally violates the slow-roll conditions for a certain duration, allowing it to climb over the barrier and continue the slow-roll inflation. Such an evolution will lead to interesting observable effects on the primordial perturbations.

Following [95], we use the action

$$S = \int d^4x \sqrt{-g} \left[ \frac{M_p^2}{2} R - M_p^2 g_1(\phi) X/2 + g_2(\phi) X^2/4 - M_p^4 V(\phi) + L_{\delta g^{00} R^{(3)}} \right], \quad (1)$$

where  $\phi$  is a dimensionless scalar field,  $X = \nabla_\mu \phi \nabla^\mu \phi$ , the EFT operator  $L_{\delta g^{00} R^{(3)}}$  is adopted to thoroughly eliminate the ghost and gradient instabilities of the primordial scalar perturbations, see, e.g., [77] for details. For simplicity, we will focus on the primordial GWs in this paper.

The background equations can be obtained as

$$3H^2 M_p^2 = \frac{M_p^2}{2} g_1 \dot{\phi}^2 + \frac{3}{4} g_2 \dot{\phi}^4 + M_p^4 V, \quad (2)$$

$$\dot{H} M_p^2 = -\frac{M_p^2}{2} g_1 \dot{\phi}^2 - \frac{1}{2} g_2 \dot{\phi}^4, \quad (3)$$

$$0 = \left( g_1 + \frac{3g_2 \dot{\phi}^2}{M_p^2} \right) \ddot{\phi} + 3g_1 H \dot{\phi} + \frac{1}{2} g_{1,\phi} \dot{\phi}^2 + \frac{3g_2 H \dot{\phi}^3}{M_p^2} + \frac{3g_{2,\phi} \dot{\phi}^4}{4M_p^2} + M_p^2 V_{,\phi}, \quad (4)$$

where “ $,\phi \equiv d/d\phi$ ”, a dot denotes the derivative with respect to the comic time  $t$ . In the background equations (2) to (4), only two of them are independent.

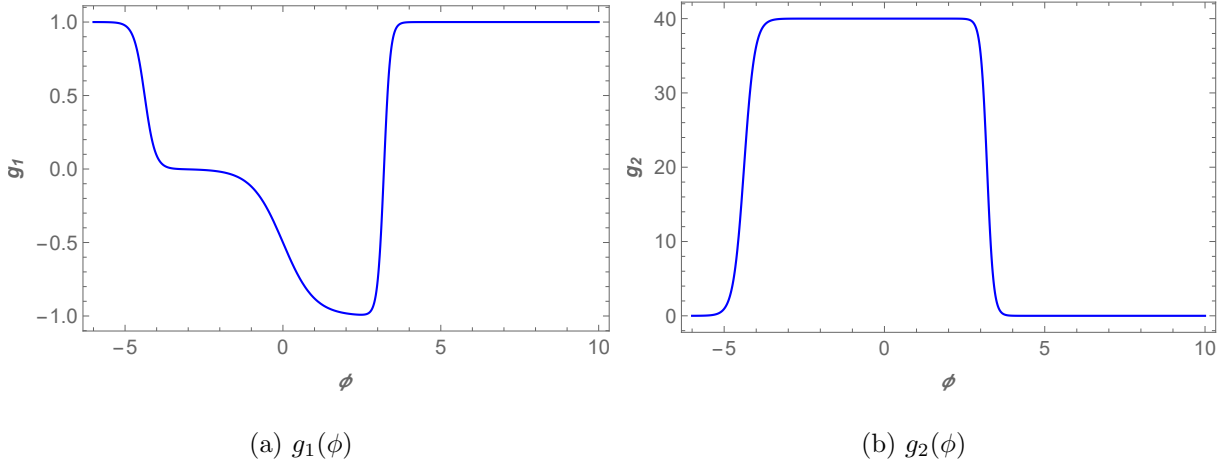


FIG. 1: The functions  $g_1(\phi)$  and  $g_2(\phi)$ , where we have set  $q_1 = 10$ ,  $q_2 = 6$ ,  $q_3 = 10$ ,  $\phi_0 = 3.2$ ,  $\phi_3 = -4.38$ ,  $f_1 = 1$ ,  $f_2 = 40$ .

To achieve the aforementioned background evolution via NEC violation, we set these  $\phi$ -dependent functions  $g_1$ ,  $g_2$  and the potential  $V$  in action (1) as

$$g_1(\phi) = \frac{1}{1 + e^{q_2(\phi - \phi_3)}} - \frac{f_1 e^{2\phi}}{1 + f_1 e^{2\phi}} + \frac{2}{1 + e^{-q_1(\phi - \phi_0)}}, \quad (5)$$

$$g_2(\phi) = \frac{f_2}{1 + e^{-q_2(\phi - \phi_3)}} \frac{1}{1 + e^{q_3(\phi - \phi_0)}}, \quad (6)$$

$$\begin{aligned} V(\phi) = & \frac{1}{2} m^2 (\phi - \phi_4)^2 \frac{1}{1 + e^{q_2(\phi - \phi_2)}} + \lambda \left[ 1 - \frac{(\phi - \phi_1)^2}{\sigma^2} \right]^2 \frac{e^{-q_4(\phi - \phi_1)}}{(1 + e^{-q_4(\phi - \phi_1)})^2} \\ & + \frac{1}{2} m^2 (\phi - \phi_5)^2 \frac{1}{1 + e^{-q_4(\phi - \phi_1)}}, \end{aligned} \quad (7)$$

where  $\lambda$ ,  $m$ ,  $f_{1,2}$ ,  $q_{1,2,3,4}$  and  $\phi_{0,1,2,3,4,5}$  are dimensionless constants. We plot  $g_1(\phi)$ ,  $g_2(\phi)$  and  $V(\phi)$  for appropriate values of these parameters in Figs. 1 and 2. As the scalar field rolls along the potential from left to right, the universe sequentially experiences the first stage of slow-roll inflation, NEC violation, and the second stage of slow-roll inflation. These two slow-roll stages are labeled as “infl” and “inf2” respectively.

The parameters introduced above should satisfy  $\phi_3 < \phi_2 < 0 < \phi_1 < \phi_0$ . As can be seen in Figs. 1 and 2, when  $\phi$  is much smaller than  $\phi_3$ ,  $g_1 = 1$  and  $g_2 = 0$ , rendering the potential responsible for the first stage of slow-roll inflation. In this regime, the first term of the potential predominates. Conversely, as  $\phi$  greatly exceeds  $\phi_0$ ,  $g_1 = 1$  and  $g_2 = 0$ , and the potential is responsible for the second stage of slow-roll inflation, with the third term in the potential becoming dominant. The exponential term in each expression serves to modulate the dominance of various terms across different regions of the potential.

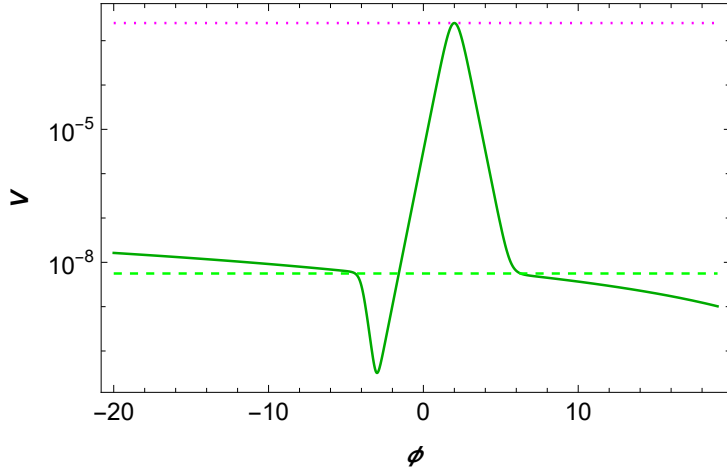


FIG. 2: A plot illustrating the potential  $V(\phi)$  with parameters set as follows:  $\phi_1 = 2$ ,  $\phi_2 = -4$ ,  $\phi_4 = 20$ ,  $\phi_5 = 29$ ,  $q_2 = 6$ ,  $q_4 = 4$ ,  $\lambda = 0.01$ ,  $\sigma = 23$ , and  $m = -4.5 \times 10^{-6}$ . The height of the potential barrier significantly exceeds that of both sides where slow-roll inflation occurs, i.e.,  $V_{\text{top}} \gg V_{\text{infl1}}$  and  $V_{\text{infl2}}$ . As the scalar field rolls along the potential from left to right, the universe sequentially experiences the first stage of slow-roll inflation, NEC violation, and the second stage of slow-roll inflation.

From Fig. 2, it can be observed that the height of the potential barrier significantly exceeds that of both sides where slow-roll inflation occurs. For a slowly rolling canonical scalar field, such a high barrier is insurmountable. However, with the action described in Eq. (1) and via the NEC violation mechanism, the scalar field can naturally disrupt the slow-roll conditions and rapidly climb over the barrier.

We numerically solve the background evolutions and display the evolutions of  $\phi$ ,  $\dot{\phi}$ ,  $H$ ,  $(aH)^{-1}$  and  $\epsilon \equiv -\dot{H}/H^2$  in Figs. 3, 4 and 5. From these figures, we can see that the universe sequentially experiences the first stage of slow-roll inflation, NEC violation, and the second stage of slow-roll inflation. This background evolution is similar to that in the scenario described in [95]. The main difference from the model in [95] lies in the fact that in this model, the energy scales of the first and second stages of slow-roll inflation are closer to each other.

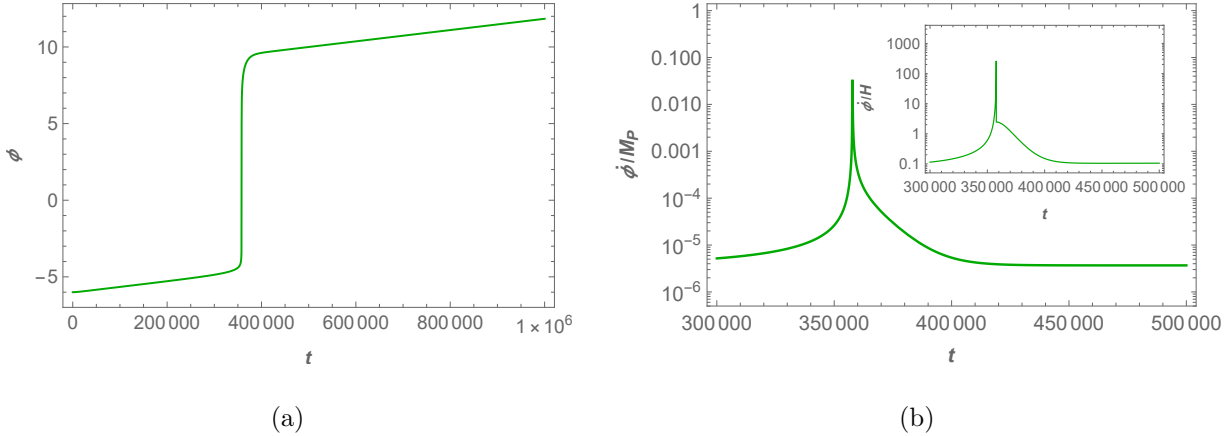


FIG. 3: The evolutions of  $\phi(t)$  (left panel) and  $\dot{\phi}$  (right panel), where  $\phi(t_{\text{ini}}) = -6$ ,  $\dot{\phi}(t_{\text{ini}}) = 0$ ,  $t_{\text{ini}} = 0$ ,  $\phi_0 = 3.2$ ,  $\phi_1 = 2$ ,  $\phi_2 = -4$ ,  $\phi_3 = -4.38$ ,  $q_1 = 10$ ,  $q_2 = 6$ ,  $q_3 = 10$ ,  $q_4 = 4$ ,  $f_1 = 1$ ,  $f_2 = 40$ ,  $\lambda = 0.01$ ,  $\sigma = 23$  and  $m = -4.5 \times 10^{-6}$ .

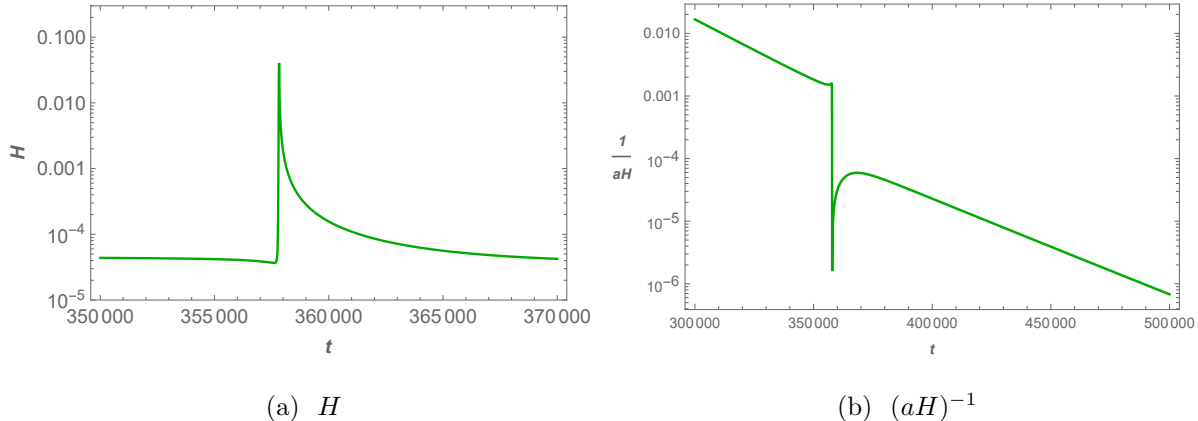


FIG. 4: The evolutions of  $H$  (left panel) and the conformal Hubble horizon  $(aH)^{-1}$  (right panel).

### III. THE POWER SPECTRUM OF PRIMORDIAL GWs

In this section, we calculate the power spectrum of primordial GWs for our model. The quadratic actions of tensor perturbation mode  $\gamma_{ij}$  can be given as

$$S_{\gamma}^{(2)} = \frac{M_p^2}{8} \int d^4x a^3 \left[ \dot{\gamma}_{ij}^2 - \frac{(\partial_k \gamma_{ij})^2}{a^2} \right]. \quad (8)$$

In the momentum space,

$$\gamma_{ij}(\tau, \mathbf{x}) = \int \frac{d^3k}{(2\pi)^3} e^{-i\mathbf{k}\cdot\mathbf{x}} \sum_{\lambda=+,\times} \hat{\gamma}_\lambda(\tau, \mathbf{k}) \epsilon_{ij}^{(\lambda)}(\mathbf{k}), \quad (9)$$

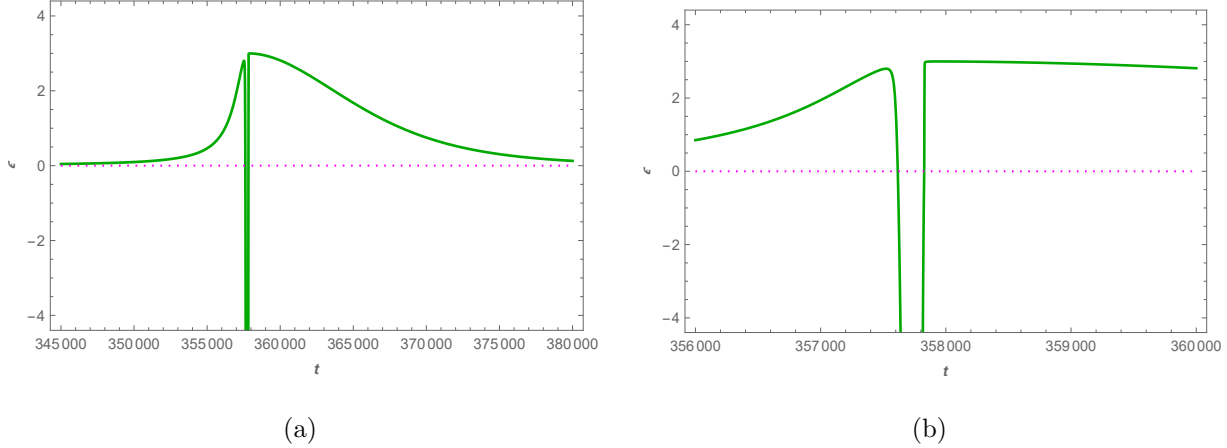


FIG. 5: The evolution of  $\epsilon = -\dot{H}/H^2$ . We have  $0 < \epsilon \ll 1$  during the first and second stages of slow-roll inflation, and  $\epsilon \ll -1$  during the NEC-violating stage.

where  $\hat{\gamma}_\lambda(\tau, \mathbf{k}) = \gamma_\lambda(\tau, k)a_\lambda(\mathbf{k}) + \gamma_\lambda^*(\tau, -k)a_\lambda^\dagger(-\mathbf{k})$ ,  $\epsilon_{ij}^{(\lambda)}(\mathbf{k})$  satisfies  $k_j\epsilon_{ij}^{(\lambda)}(\mathbf{k}) = 0$ ,  $\epsilon_{ii}^{(\lambda)}(\mathbf{k}) = 0$ ,  $\epsilon_{ij}^{(\lambda)}(\mathbf{k})\epsilon_{ij}^{*(\lambda')}(\mathbf{k}) = \delta_{\lambda\lambda'}$  and  $\epsilon_{ij}^{*(\lambda)}(\mathbf{k}) = \epsilon_{ij}^{(\lambda)}(-\mathbf{k})$ ;  $a_\lambda(\mathbf{k})$  and  $a_\lambda^\dagger(\mathbf{k}')$  satisfy  $[a_\lambda(\mathbf{k}), a_{\lambda'}^\dagger(\mathbf{k}')] = \delta_{\lambda\lambda'}\delta^{(3)}(\mathbf{k} - \mathbf{k}')$ .

Using the Eq. (8), we can obtain the equation of motion for  $\gamma_\lambda(\tau, \mathbf{k})$  as

$$u_k'' + \left( k^2 - \frac{a''}{a} \right) u_k = 0, \quad (10)$$

where  $u_k \equiv \gamma_\lambda(\tau, k) a M_p / 2$  and a prime denotes  $d/d\tau$ . The power spectrum of primordial GWs is defined as

$$P_T = \frac{k^3}{2\pi^2} \sum_{\lambda=+,\times} |\gamma_\lambda|^2 = \frac{4k^3}{\pi^2 M_p^2} \cdot \frac{|u_k|^2}{a^2}, \quad (11)$$

which should be evaluated at the end of the second stage of slow-roll inflation.

We numerically solve Eq. (10) and obtain the power spectrum of primordial GWs for our model. The results are displayed in Fig. 6. We observe a significant enhancement in the power spectrum amplitude of perturbation modes that exit the horizon around the NEC violation epoch in this model. This is because perturbation modes that are outside the horizon during the NEC violation period experience rapid growth, surpassing the amplitude of the constant mode. Therefore, the power spectrum at intermediate scales exhibits a blue tilt. Similar to the model in Ref. [95], the model in this paper also has the potential to explain observations at the PTA scale. However, unlike the model in Ref. [95], the power spectrum amplitudes of perturbation modes that exit the horizon during the second stage of slow-roll inflation are not significantly different from those that exit during the first stage.

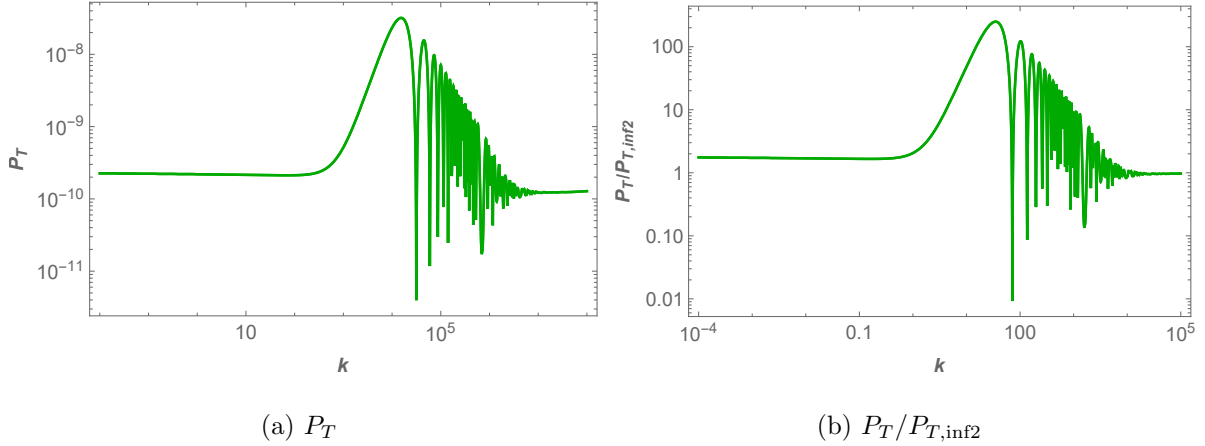


FIG. 6: The power spectra  $P_T$  of primordial GWs for our model obtained by numerically solving Eq. (10). We have set  $q_1 = 10$ ,  $q_2 = 6$ ,  $q_3 = 10$ ,  $q_4 = 4$ ,  $\phi_0 = 3.2$ ,  $\phi_1 = 2$ ,  $\phi_2 = -4$ ,  $\phi_3 = -4.38$ ,  $\phi_4 = 20$ ,  $\phi_5 = 29$ ,  $f_1 = 1$ ,  $f_2 = 40$ ,  $\lambda = 0.01$ ,  $\sigma = 23$ ,  $m = -4.5 \times 10^{-6}$ ,  $\dot{\phi}(t_{\text{ini}}) = -6$ ,  $\ddot{\phi}(t_{\text{ini}}) = 0$  and  $t_{\text{ini}} = 0$ .

In the following, we attempt to provide an analytical derivation of the power spectrum. Analogous to the approach in Ref. [95], we divide the background evolution in this model into four stages, with the scale factor of the  $j$ -th stage approximately parameterized as

$$a_j(\tau) \sim (\tau_{R,j} - \tau)^{\frac{1}{\epsilon_j - 1}}, \quad (12)$$

where  $\epsilon_j \equiv -\dot{H}_j/H_j^2 = \frac{3}{2}(1 + w_j)$ ,  $\tau_{R,j} \equiv \tau_j - (\epsilon_j - 1)^{-1}\mathcal{H}^{-1}(\tau_j)$ ,  $j = 1, 2, 3, 4$ . For simplicity, we assume  $\epsilon_j$  (i.e., the equation of state parameter  $w_j$ ) as a constant. We also require continuity of  $a$  and  $a'$  at each transition moment.

With Eq. (12), we have

$$\frac{a''_j}{a_j} = \frac{\nu_j^2 - 1/4}{(\tau - \tau_{R,j})^2}, \quad (13)$$

where  $\nu_j = \frac{3}{2} \left| \frac{1-w_j}{1+3w_j} \right|$ . Consequently, the solutions to Eq. (10) for each phase can be given as

$$\begin{aligned} u_{k,1}(\tau) &= \frac{\sqrt{\pi(\tau_{R,1} - \tau)}}{2} \left\{ \alpha_1 H_{\nu_1}^{(1)}[k(\tau_{R,1} - \tau)] + \beta_1 H_{\nu_1}^{(2)}[k(\tau_{R,1} - \tau)] \right\}, \quad (\tau < \tau_1), \\ u_{k,2}(\tau) &= \frac{\sqrt{\pi(\tau_{R,2} - \tau)}}{2} \left\{ \alpha_2 H_{\nu_2}^{(1)}[k(\tau_{R,2} - \tau)] + \beta_2 H_{\nu_2}^{(2)}[k(\tau_{R,2} - \tau)] \right\}, \quad (\tau_1 \leq \tau \leq \tau_2), \\ u_{k,3}(\tau) &= \frac{\sqrt{\pi(\tau_{R,3} - \tau)}}{2} \left\{ \alpha_3 H_{\nu_3}^{(1)}[k(\tau_{R,3} - \tau)] + \beta_3 H_{\nu_3}^{(2)}[k(\tau_{R,3} - \tau)] \right\}, \quad (\tau_2 < \tau \leq \tau_3), \\ u_{k,4}(\tau) &= \frac{\sqrt{\pi(\tau_{R,4} - \tau)}}{2} \left\{ \alpha_4 H_{\nu_4}^{(1)}[k(\tau_{R,4} - \tau)] + \beta_4 H_{\nu_4}^{(2)}[k(\tau_{R,4} - \tau)] \right\}, \quad (\tau_3 < \tau \leq \tau_4), \end{aligned} \quad (14)$$

where  $\alpha_j$  and  $\beta_j$  are  $k$ -dependent coefficients,  $j = 1, 2, 3, 4$ . We set the initial state as the Bunch-Davis vacuum, i.e.,  $u_k = e^{-ik\tau}/\sqrt{2k}$ , which indicates that  $|\alpha_1| = 1$  and  $|\beta_1| = 0$ .

Using the matching conditions  $u_{k,j}(\tau_j) = u_{k,j+1}(\tau_j)$  and  $u'_{k,j}|_{\tau=\tau_j} = u'_{k,j+1}|_{\tau=\tau_j}$ , we can obtain all of the  $\alpha_j$  and  $\beta_j$  for  $j = 2, 3, 4$ . We have

$$\begin{pmatrix} \alpha_{j+1} \\ \beta_{j+1} \end{pmatrix} = \mathcal{M}^{(j)} \begin{pmatrix} \alpha_j \\ \beta_j \end{pmatrix}, \quad \text{where } \mathcal{M}^{(j)} = \begin{pmatrix} \mathcal{M}_{11}^{(j)} & \mathcal{M}_{12}^{(j)} \\ \mathcal{M}_{21}^{(j)} & \mathcal{M}_{22}^{(j)} \end{pmatrix}, \quad (15)$$

The details of the matrix elements of the transfer matrix can be found in [102, 103]. At the end of the second slow-roll inflation, the power spectrum can be given as

$$P_T = \frac{4k^3}{\pi^2 M_p^2} \cdot \left. \frac{|u_{k,4}|^2}{a^2} \right|_{\tau \rightarrow \tau_4} = P_{T,\text{inf2}} |\alpha_4 - \beta_4|^2, \quad (16)$$

where  $P_{T,\text{inf2}} = \frac{2H_{\text{inf2}}^2}{\pi^2 M_p^2}$ . A detailed expression for  $\alpha_4$  and  $\beta_4$  can be found in Appendix A. We plot  $P_T/P_{T,\text{inf2}} = |\alpha_4 - \beta_4|^2$  in Fig. 7 for different choices of  $w_i$ . We can see from Figs. 6(b) and 7(a) that the approximation works well for our model with appropriate choices of  $w_i$ . In our parameterization, the height difference between the two platforms in the potential can be adjusted by changing  $\epsilon_3 = -\dot{H}/H^2 = \frac{3}{2}(1 + w_j)$ .

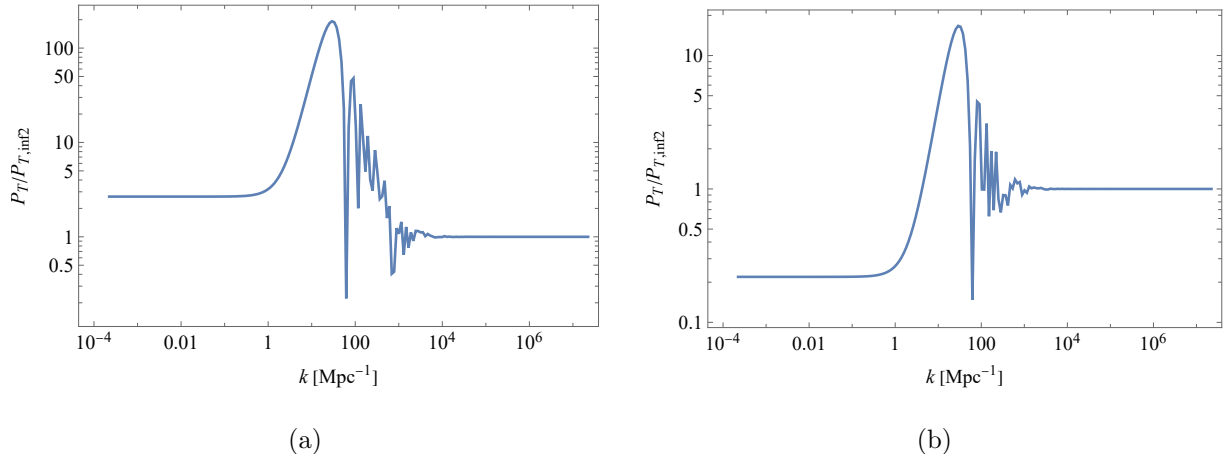


FIG. 7: The power spectrum of the primordial GWs given by Eq. (16). For the left panel, we set  $w_1 = -1$ ,  $w_2 = -10$ ,  $w_3 = 1$ , and  $w_4 = -1$ , providing a close approximation to the result shown in Fig. 6(b). In the right panel, we choose  $w_1 = -1$ ,  $w_2 = -10$ ,  $w_3 = 2/3$ , and  $w_4 = -1$ , resembling the scenario discussed in Ref. [95].

#### IV. THE ENERGY DENSITY SPECTRUM OF GWs

The energy density spectrum of GWs [104, 105] (see also [54, 106]) is

$$\Omega_{GW}(\tau_0) = \frac{k^2}{12a_0^2 H_0^2} P_T(k) \left[ \frac{3\Omega_m j_1(k\tau_0)}{k\tau_0} \sqrt{1.0 + 1.36 \frac{k}{k_{\text{eq}}} + 2.50 \left( \frac{k}{k_{\text{eq}}} \right)^2} \right]^2, \quad (17)$$

where  $H_0 = 67.8 \text{ km/s/Mpc}$ ,  $\tau_0 = 1.41 \times 10^4 \text{ Mpc}$ ,  $a_0 = 1$ ,  $k_{\text{eq}} = 0.073 \Omega_m h^2 \text{ Mpc}^{-1}$  is the wavenumber corresponding to the mode that entered the horizon at the equality of matter and radiation,  $\Omega_m = \rho_m/\rho_c$  is the density fraction of matter today,  $\rho_c = 3H_0^2/(8\pi G)$  is the critical energy density, and  $j_1(x)$  is the spherical Bessel function of the first kind. We plot the energy density spectrum of GWs for our model in Figs. 8(a) and 8(b), using both the numerical results obtained by solving Eq. (10) and the analytical results provided by Eq. (16), respectively. Namely, Figs. 8(a) and 8(b) correspond to the power spectra displayed in Figs. 6(a) and 7(a), respectively.

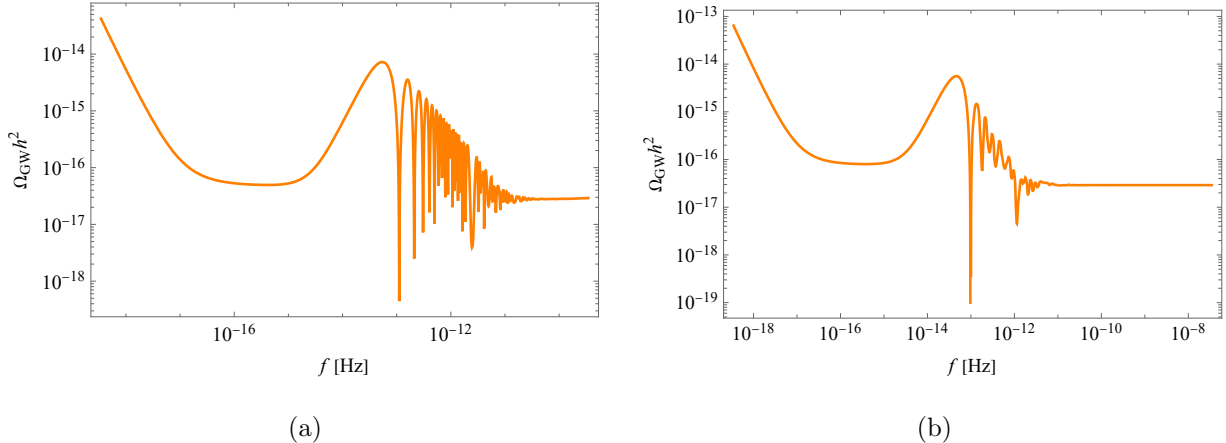


FIG. 8: The energy density spectrum of GWs for our model obtained by using both the numerical results obtained by solving Eq. (10) (left panel) and the analytical results provided by Eq. (16) (right panel).

Comparing Figs. 8(a) and 8(b), we observe a good agreement between the energy density spectra obtained by the two methods. In the second case, where the slow-roll parameters are approximated as constants, some details of the mode evolution are not fully reflected. For observational purposes, the distinctive features may include the blue-tilted nature in the middle-frequency range and the decreasing amplitude of these oscillations at higher frequencies.

## V. CONCLUSION

In this paper, we propose a new single-field model where the universe sequentially undergoes a first stage of slow-roll inflation, NEC violation, and a second stage of slow-roll inflation. Within the potential responsible for slow-roll inflation, there exists a high barrier, over which the rolling inflaton climb via the NEC violation mechanism before entering the second inflationary stage. Following the NEC violation, there is a process of energy scale reduction, resulting in the energy scales of the two slow-roll inflation stages being relatively close, contrasting with the model in [95].

We calculate the power spectrum of primordial GWs using both numerical and analytical methods, comparing the results obtained from these two approaches. We find that the approximation used in the analytical derivation closely matches the results from numerical calculations. The power spectrum is nearly scale-invariant on both large and small scales. However, in the middle-frequency range, it shows a blue-tilted nature, while at higher frequencies, there is a reduction in oscillation amplitudes. These unique characteristics could potentially differentiate our model from others.

In the early universe, NEC violation may have occurred multiple times. We present a sketch of the GW power spectrum in Fig. 9 for the scenario where  $\phi$  climbs over the potential barriers multiple times. The accumulation of future observational data from various frequency bands, including CMB, PTA, Advanced LIGO, Advanced Virgo, LISA, Taiji and Tianqin, will enable more tests or constraints on NEC violation in the very early universe.

### Acknowledgments

Y. C. is supported in part by the National Natural Science Foundation of China (Grant No. 11905224), the China Postdoctoral Science Foundation (Grant No. 2021M692942) and Zhengzhou University (Grant Nos. 32213984, 35220136). Y.-S. P. is supported by NSFC, No.12075246, National Key Research and Development Program of China, No. 2021YFC2203004, and the Fundamental Research Funds for the Central Universities.

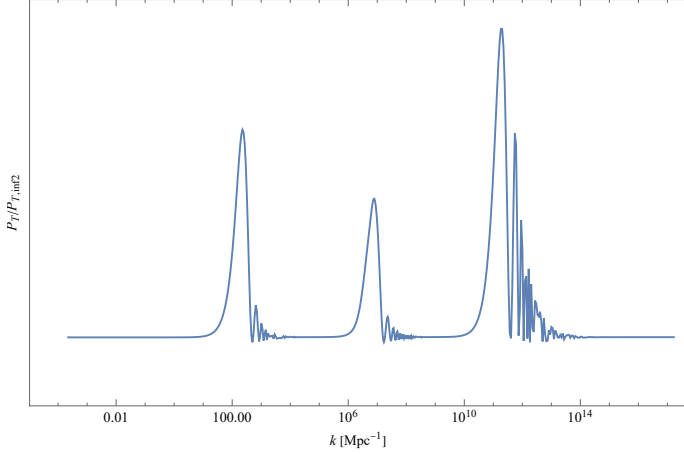


FIG. 9: A sketch of the GW power spectrum for the scenario where  $\phi$  climbs over the potential barriers multiple times.

### Appendix A: Detailed analytic expression of $\alpha$ and $\beta$

The scale factor can be parameterized as a piecewise function of  $\tau$ , i.e.,

$$a_j(\tau) = a_j(\tau_j) \left( \frac{\tau - \tau_{R,j}}{\tau_j - \tau_{R,j}} \right)^{\frac{1}{\epsilon_j - 1}}, \quad \tau < \tau_j. \quad (\text{A1})$$

The continuity of  $a$  gives

$$a_1(\tau_1) = a_2(\tau_2) \left( \frac{\tau_1 - \tau_{R,2}}{\tau_2 - \tau_{R,2}} \right)^{\frac{1}{\epsilon_2 - 1}}, \quad (\text{A2})$$

$$a_2(\tau_2) = a_3(\tau_3) \left( \frac{\tau_2 - \tau_{R,3}}{\tau_3 - \tau_{R,3}} \right)^{\frac{1}{\epsilon_3 - 1}}, \quad (\text{A3})$$

$$a_3(\tau_3) = a_4(\tau_4) \left( \frac{\tau_3 - \tau_{R,4}}{\tau_4 - \tau_{R,4}} \right)^{\frac{1}{\epsilon_4 - 1}}. \quad (\text{A4})$$

Considering the continuity of  $a'$  or  $\mathcal{H}$ , we can define the following quantities:

$$\bar{\mathcal{H}}_1 \equiv \mathcal{H}(\tau_1), \quad \bar{\mathcal{H}}_2 \equiv \mathcal{H}(\tau_2), \quad \bar{\mathcal{H}}_3 \equiv \mathcal{H}(\tau_3). \quad (\text{A5})$$

Using (A1), we can obtain the integration constants  $\tau_{R,j}$  as

$$\tau_{R,1} = \tau_1 + \bar{\mathcal{H}}_1^{-1}, \quad \tau_{R,2} = \tau_1 + (v_2 - \frac{1}{2})\bar{\mathcal{H}}_1^{-1}, \quad \tau_{R,3} = \tau_2 + (v_3 - \frac{1}{2})\bar{\mathcal{H}}_2^{-1}, \quad (\text{A6})$$

$$\tau_{R,3} = \tau_2 + (-v_3 - \frac{1}{2})\bar{\mathcal{H}}_2^{-1}, \quad \tau_{R,4} = \tau_3 + \bar{\mathcal{H}}_3^{-1}, \quad (\text{A7})$$

where  $\nu_j = \frac{3}{2} \left| \frac{1-w_j}{1+3w_j} \right|$ , and  $\epsilon_j = \frac{3}{2}(1+w_j) \simeq \text{const.}$ . Note that for  $-\frac{1}{3} < w_j < 1$  and  $w_j < -\frac{1}{3}$ , we have  $\nu_j = -\frac{1}{2} - \frac{1}{1-\epsilon_j}$  and  $\nu_j = \frac{1}{2} + \frac{1}{1-\epsilon_j}$ , respectively.

Using the matching method, we obtain the following recursive relations:

$$\begin{aligned} \alpha_2 &= \frac{i\pi}{8x_1} \sqrt{\frac{x_1}{x_2}} \left( H_{\frac{3}{2}}^{(1)}(x_1) \left( 2x_1 x_2 H_{\nu_2-1}^{(2)}(x_2) + (-2\nu_2 x_1 + x_1 + 2x_2) H_{\nu_2}^{(2)}(x_2) \right) \right. \\ &\quad \left. - 2x_1 x_2 H_{\frac{1}{2}}^{(1)}(x_1) H_{\nu_2}^{(2)}(x_2) \right), \end{aligned} \quad (\text{A8})$$

$$\begin{aligned} \beta_2 &= -\frac{i\pi}{8x_1} \sqrt{\frac{x_1}{x_2}} \left( H_{\frac{3}{2}}^{(1)}(x_1) \left( 2x_1 x_2 H_{\nu_2-1}^{(1)}(x_2) + (-2\nu_2 x_1 + x_1 + 2x_2) H_{\nu_2}^{(1)}(x_2) \right) \right. \\ &\quad \left. - 2x_1 x_2 H_{\frac{1}{2}}^{(1)}(x_1) H_{\nu_2}^{(1)}(x_2) \right), \end{aligned} \quad (\text{A9})$$

$$\begin{aligned} \alpha_3 &= -\frac{\pi}{8y_1} \sqrt{-\frac{y_1}{y_2}} \left( y_2 H_{\nu_3}^{(2)}(y_2) \left( 2\alpha_2 y_1 H_{\nu_2-1}^{(1)}(y_1) + (\alpha_2 - 2\alpha_2 \nu_2) H_{\nu_2}^{(1)}(y_1) \right. \right. \\ &\quad + 2\beta_2 y_1 H_{\nu_2-1}^{(2)}(y_1) + (\beta_2 - 2\beta_2 \nu_2) H_{\nu_2}^{(2)}(y_1) \\ &\quad \left. \left. - y_1 \left( 2y_2 H_{\nu_3-1}^{(2)}(y_2) + (1 - 2\nu_3) H_{\nu_3}^{(2)}(y_2) \right) \cdot \left( \alpha_2 H_{\nu_2}^{(1)}(y_1) + \beta_2 H_{\nu_2}^{(2)}(y_1) \right) \right) \right), \end{aligned} \quad (\text{A10})$$

$$\begin{aligned} \beta_3 &= \frac{\pi}{8y_1} \sqrt{-\frac{y_1}{y_2}} \left( 2\alpha_2 y_1 y_2 H_{\nu_2-1}^{(1)}(y_1) H_{\nu_3}^{(1)}(y_2) \right. \\ &\quad + \alpha_2 H_{\nu_2}^{(1)}(y_1) \left( (2\nu_3 y_1 - 2\nu_2 y_2 - y_1 + y_2) H_{\nu_3}^{(1)}(y_2) - 2y_1 y_2 H_{\nu_3-1}^{(1)}(y_2) \right) \\ &\quad - 2\beta_2 y_1 y_2 H_{\nu_3-1}^{(1)}(y_2) H_{\nu_2}^{(2)}(y_1) + \beta_2 H_{\nu_3}^{(1)}(y_2) \left( 2y_1 y_2 H_{\nu_2-1}^{(2)}(y_1) \right. \\ &\quad \left. \left. + (2\nu_3 y_1 - 2\nu_2 y_2 - y_1 + y_2) H_{\nu_2}^{(2)}(y_1) \right) \right), \end{aligned} \quad (\text{A11})$$

$$\begin{aligned} \alpha_4 &= \frac{\pi}{8z_1} \sqrt{-\frac{z_1}{z_2}} \left( 2z_1 \left( H_{\frac{3}{2}}^{(2)}(z_2) - z_2 H_{\frac{1}{2}}^{(2)}(z_2) \right) \left( \alpha_3 H_{\nu_3}^{(1)}(z_1) + \beta_3 H_{\nu_3}^{(2)}(z_1) \right) \right. \\ &\quad + z_2 H_{\frac{3}{2}}^{(2)}(z_2) \left( 2\alpha_3 z_1 H_{\nu_3-1}^{(1)}(z_1) + (\alpha_3 - 2\alpha_3 \nu_3) H_{\nu_3}^{(1)}(z_1) \right. \\ &\quad \left. \left. + 2\beta_3 z_1 H_{\nu_3-1}^{(2)}(z_1) + (\beta_3 - 2\beta_3 \nu_3) H_{\nu_3}^{(2)}(z_1) \right) \right), \end{aligned} \quad (\text{A12})$$

$$\begin{aligned} \beta_4 &= -\frac{\pi}{8z_1} \sqrt{-\frac{z_1}{z_2}} \left( H_{\frac{3}{2}}^{(1)}(z_2) \left( 2\alpha_3 z_1 z_2 H_{\nu_3-1}^{(1)}(z_1) \right. \right. \\ &\quad + \alpha_3 (-2\nu_3 z_2 + 2z_1 + z_2) H_{\nu_3}^{(1)}(z_1) \\ &\quad \left. \left. + 2\beta_3 z_1 z_2 H_{\nu_3-1}^{(2)}(z_1) + \beta_3 (-2\nu_3 z_2 + 2z_1 + z_2) H_{\nu_3}^{(2)}(z_1) \right) \right. \\ &\quad \left. - 2z_1 z_2 H_{\frac{1}{2}}^{(1)}(z_2) \left( \alpha_3 H_{\nu_3}^{(1)}(z_1) + \beta_3 H_{\nu_3}^{(2)}(z_1) \right) \right), \end{aligned} \quad (\text{A13})$$

where  $x_1 = k(\tau_{R,1} - \tau_1)$ ,  $x_2 = k(\tau_{R,2} - \tau_1)$ ,  $y_1 = k(\tau_{R,2} - \tau_2)$ ,  $y_2 = k(\tau_{R,3} - \tau_2)$ ,  $z_1 = k(\tau_{R,3} - \tau_3)$ ,  $z_2 = k(\tau_{R,4} - \tau_3)$ . Since the results are too complex, we only provide the recursive formulas for  $\alpha_j$  and  $\beta_j$ .

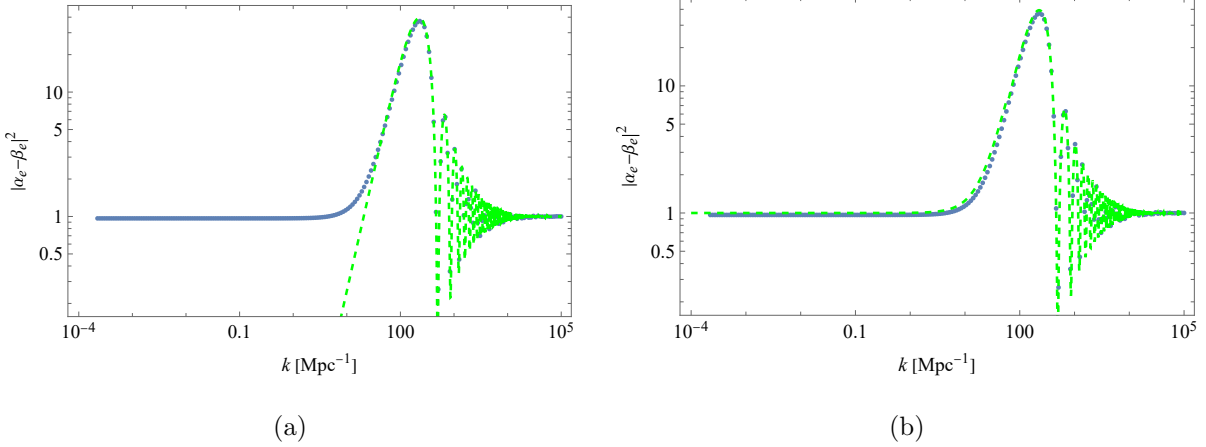


FIG. 10: Left: Comparison between  $|G_1|^2$  (green dashed curve) and the numerical result of  $P_T/P_{T,inf2}$  (blue dotted curve). Right: Comparison between the template (A15) (green dashed curve) and the numerical result of  $P_T/P_{T,inf2}$  (blue dotted curve). We have set  $\bar{\mathcal{H}}_1 = 10^4 a_0 H_0$ , where  $a_0 = 1$  and  $H_0 = 67 \text{ km/s/Mpc}$ . We also set  $w_2 = -15$  and  $w_3 = 2/3$ , which corresponding to  $\nu_2 = 6/11$  and  $\nu_3 = 1/6$ , respectively.

Next, we attempt to explore potential approximations. It's worth noting that in our model,  $y_2$  and  $z_1$  are negative. Therefore, our approach here is to consider  $k \gg \bar{\mathcal{H}}_1$ . By

series expansion, we get

$$\begin{aligned}
G_1 &= \alpha_4 - \beta_4 \\
&= \frac{\pi^{3/2}}{16\sqrt{2}z_2^2} \left( 2H_{\nu_2-1}^{(1)}(y_1) \left( H_{\nu_3}^{(1)}(y_2) \left( 2H_{\nu_3-1}^{(2)}(z_1) \sqrt{y_1y_2z_1} z_2 (\cos(z_2) z_2 - \sin(z_2)) \right. \right. \right. \\
&\quad + H_{\nu_3}^{(2)}(z_1) \left( \sin(z_2) \left( 2\sqrt{y_1y_2z_1} z_2^2 + \sqrt{\frac{y_1y_2}{z_1}} (1 - 2\nu_3) z_2 - 2\sqrt{y_1y_2z_1} \right) \right. \\
&\quad \left. \left. \left. + \cos(z_2) z_2 \left( \sqrt{\frac{y_1y_2}{z_1}} z_2 (2\nu_3 - 1) + 2\sqrt{y_1y_2z_1} \right) \right) \right) \\
&\quad + H_{\nu_3}^{(2)}(y_2) \left( H_{\nu_3}^{(1)}(z_1) \left( \sin(z_2) \left( -2\sqrt{y_1y_2z_1} z_2^2 + \sqrt{\frac{y_1y_2}{z_1}} (2\nu_3 - 1) z_2 + 2\sqrt{y_1y_2z_1} \right) \right. \right. \\
&\quad \left. \left. - \cos(z_2) z_2 \left( \sqrt{\frac{y_1y_2}{z_1}} z_2 (2\nu_3 - 1) + 2\sqrt{y_1y_2z_1} \right) \right) - 2H_{\nu_3-1}^{(1)}(z_1) \sqrt{y_1y_2z_1} z_2 (\cos(z_2) z_2 \right. \\
&\quad \left. \left. - \sin(z_2)) \right) \right) + H_{\nu_2}^{(1)}(y_1) \left( -4\cos(z_2) H_{\nu_3}^{(1)}(y_2) H_{\nu_3}^{(2)}(z_1) \sqrt{\frac{y_1}{y_2z_1}} \nu_3^2 z_2^2 \right. \\
&\quad \left. + 2\cos(z_2) H_{\nu_3}^{(1)}(y_2) H_{\nu_3}^{(2)}(z_1) \sqrt{\frac{y_2}{y_1z_1}} \nu_2 z_2^2 - 4\cos(z_2) H_{\nu_3}^{(1)}(y_2) H_{\nu_3-1}^{(2)}(z_1) \sqrt{\frac{y_2z_1}{y_1}} \nu_2 z_2^2 \right. \\
&\quad \left. - 4H_{\nu_3}^{(1)}(y_2) H_{\nu_3}^{(2)}(z_1) \sin(z_2) \sqrt{\frac{y_2z_1}{y_1}} \nu_2 z_2^2 - 4\cos(z_2) H_{\nu_3}^{(1)}(y_2) H_{\nu_3}^{(2)}(z_1) \sqrt{\frac{y_2}{y_1z_1}} \nu_2 \nu_3 z_2^2 \right. \\
&\quad \left. + 4\cos(z_2) H_{\nu_3}^{(1)}(y_2) H_{\nu_3}^{(2)}(z_1) \sqrt{\frac{y_1}{y_2z_1}} \nu_3 z_2^2 + 2\cos(z_2) H_{\nu_3}^{(1)}(y_2) H_{\nu_3}^{(2)}(z_1) \sqrt{\frac{y_2}{y_1z_1}} \nu_3 z_2^2 \right. \\
&\quad \left. - 4\cos(z_2) H_{\nu_3-1}^{(1)}(y_2) H_{\nu_3}^{(2)}(z_1) \sqrt{\frac{y_1y_2}{z_1}} \nu_3 z_2^2 - 4\cos(z_2) H_{\nu_3}^{(1)}(y_2) H_{\nu_3-1}^{(2)}(z_1) \sqrt{\frac{y_1z_1}{y_2}} \nu_3 z_2^2 \right. \\
&\quad \left. - 4H_{\nu_3}^{(1)}(y_2) H_{\nu_3}^{(2)}(z_1) \sin(z_2) \sqrt{\frac{y_1z_1}{y_2}} \nu_3 z_2^2 - \cos(z_2) H_{\nu_3}^{(1)}(y_2) H_{\nu_3}^{(2)}(z_1) \sqrt{\frac{y_1}{y_2z_1}} z_2^2 \right. \\
&\quad \left. - \cos(z_2) H_{\nu_3}^{(1)}(y_2) H_{\nu_3}^{(2)}(z_1) \sqrt{\frac{y_2}{y_1z_1}} z_2^2 + 2\cos(z_2) H_{\nu_3-1}^{(1)}(y_2) H_{\nu_3}^{(2)}(z_1) \sqrt{\frac{y_1y_2}{z_1}} z_2^2 \right. \\
&\quad \left. + 2\cos(z_2) H_{\nu_3}^{(1)}(y_2) H_{\nu_3-1}^{(2)}(z_1) \sqrt{\frac{y_1z_1}{y_2}} z_2^2 + 2H_{\nu_3}^{(1)}(y_2) H_{\nu_3}^{(2)}(z_1) \sin(z_2) \sqrt{\frac{y_1z_1}{y_2}} z_2^2 \right. \\
&\quad \left. + 2\cos(z_2) H_{\nu_3}^{(1)}(y_2) H_{\nu_3-1}^{(2)}(z_1) \sqrt{\frac{y_2z_1}{y_1}} z_2^2 + 2H_{\nu_3}^{(1)}(y_2) H_{\nu_3}^{(2)}(z_1) \sin(z_2) \sqrt{\frac{y_2z_1}{y_1}} z_2^2 \right. \\
&\quad \left. - 4\cos(z_2) H_{\nu_3-1}^{(1)}(y_2) H_{\nu_3-1}^{(2)}(z_1) \sqrt{y_1y_2z_1} z_2^2 - 4H_{\nu_3-1}^{(1)}(y_2) H_{\nu_3}^{(2)}(z_1) \sin(z_2) \sqrt{y_1y_2z_1} z_2^2 \right. \\
&\quad \left. + 4H_{\nu_3}^{(1)}(y_2) H_{\nu_3}^{(2)}(z_1) \sin(z_2) \sqrt{\frac{y_1}{y_2z_1}} \nu_3^2 z_2 - 2H_{\nu_3}^{(1)}(y_2) H_{\nu_3}^{(2)}(z_1) \sin(z_2) \sqrt{\frac{y_2}{y_1z_1}} \nu_2 z_2 \right. \\
&\quad \left. - 4\cos(z_2) H_{\nu_3}^{(1)}(y_2) H_{\nu_3}^{(2)}(z_1) \sqrt{\frac{y_2z_1}{y_1}} \nu_2 z_2 + 4H_{\nu_3}^{(1)}(y_2) H_{\nu_3-1}^{(2)}(z_1) \sin(z_2) \sqrt{\frac{y_2z_1}{y_1}} \nu_2 z_2 \right. \\
&\quad \left. + 4H_{\nu_3}^{(1)}(y_2) H_{\nu_3}^{(2)}(z_1) \sin(z_2) \sqrt{\frac{y_2}{y_1z_1}} \nu_2 \nu_3 z_2 - 4H_{\nu_3}^{(1)}(y_2) H_{\nu_3}^{(2)}(z_1) \sin(z_2) \sqrt{\frac{y_1}{y_2z_1}} \nu_3 z_2 \right. \\
&\quad \left. - 2H_{\nu_3}^{(1)}(y_2) H_{\nu_3}^{(2)}(z_1) \sin(z_2) \sqrt{\frac{y_2}{y_1z_1}} \nu_3 z_2 + 4H_{\nu_3-1}^{(1)}(y_2) H_{\nu_3}^{(2)}(z_1) \sin(z_2) \sqrt{\frac{y_1y_2}{z_1}} \nu_3 z_2 \right)
\end{aligned} \tag{A14}$$

$$\begin{aligned}
& -4 \cos(z_2) H_{\nu_3}^{(1)}(y_2) H_{\nu_3}^{(2)}(z_1) \sqrt{\frac{y_1 z_1}{y_2}} \nu_3 z_2 + 4 H_{\nu_3}^{(1)}(y_2) H_{\nu_3-1}^{(2)}(z_1) \sin(z_2) \sqrt{\frac{y_1 z_1}{y_2}} \nu_3 z_2 \\
& + 2 H_{\nu_3-1}^{(1)}(z_1) (\cos(z_2) z_2 - \sin(z_2)) \left( 2 \sqrt{y_1 y_2 z_1} H_{\nu_3-1}^{(2)}(y_2) + H_{\nu_3}^{(2)}(y_2) \left( 2 \sqrt{\frac{y_2 z_1}{y_1}} \nu_2 \right. \right. \\
& \left. \left. + 2 \sqrt{\frac{y_1 z_1}{y_2}} \nu_3 - \sqrt{\frac{y_1 z_1}{y_2}} - \sqrt{\frac{y_2 z_1}{y_1}} \right) \right) z_2 + H_{\nu_3}^{(1)}(y_2) H_{\nu_3}^{(2)}(z_1) \sin(z_2) \sqrt{\frac{y_1}{y_2 z_1}} z_2 \\
& + H_{\nu_3}^{(1)}(y_2) H_{\nu_3}^{(2)}(z_1) \sin(z_2) \sqrt{\frac{y_2}{y_1 z_1}} z_2 - 2 H_{\nu_3-1}^{(1)}(y_2) H_{\nu_3}^{(2)}(z_1) \sin(z_2) \sqrt{\frac{y_1 y_2}{z_1}} z_2 \\
& + 2 \cos(z_2) H_{\nu_3}^{(1)}(y_2) H_{\nu_3}^{(2)}(z_1) \sqrt{\frac{y_1 z_1}{y_2}} z_2 - 2 H_{\nu_3}^{(1)}(y_2) H_{\nu_3-1}^{(2)}(z_1) \sin(z_2) \sqrt{\frac{y_1 z_1}{y_2}} z_2 \\
& + 2 \cos(z_2) H_{\nu_3}^{(1)}(y_2) H_{\nu_3}^{(2)}(z_1) \sqrt{\frac{y_2 z_1}{y_1}} z_2 - 2 H_{\nu_3}^{(1)}(y_2) H_{\nu_3-1}^{(2)}(z_1) \sin(z_2) \sqrt{\frac{y_2 z_1}{y_1}} z_2 \\
& - 4 \cos(z_2) H_{\nu_3-1}^{(1)}(y_2) H_{\nu_3}^{(2)}(z_1) \sqrt{y_1 y_2 z_1} z_2 + 4 H_{\nu_3-1}^{(1)}(y_2) H_{\nu_3-1}^{(2)}(z_1) \sin(z_2) \sqrt{y_1 y_2 z_1} z_2 \\
& + 4 H_{\nu_3}^{(1)}(y_2) H_{\nu_3}^{(2)}(z_1) \sin(z_2) \sqrt{\frac{y_2 z_1}{y_1}} \nu_2 + 4 H_{\nu_3}^{(1)}(y_2) H_{\nu_3}^{(2)}(z_1) \sin(z_2) \sqrt{\frac{y_1 z_1}{y_2}} \nu_3 \\
& + H_{\nu_3}^{(1)}(z_1) \left( 2 H_{\nu_3-1}^{(2)}(y_2) \left( \sin(z_2) \left( 2 \sqrt{y_1 y_2 z_1} z_2^2 + \sqrt{\frac{y_1 y_2}{z_1}} (1 - 2 \nu_3) z_2 - 2 \sqrt{y_1 y_2 z_1} \right) \right. \right. \\
& \left. \left. + \cos(z_2) z_2 \left( \sqrt{\frac{y_1 y_2}{z_1}} z_2 (2 \nu_3 - 1) + 2 \sqrt{y_1 y_2 z_1} \right) \right) + H_{\nu_3}^{(2)}(y_2) \left( \cos(z_2) z_2 \left( 4 \sqrt{\frac{y_2 z_1}{y_1}} \nu_2 \right. \right. \\
& \left. \left. + 4 \sqrt{\frac{y_1 z_1}{y_2}} \nu_3 + z_2 (2 \nu_3 - 1) \left( 2 \sqrt{\frac{y_2}{y_1 z_1}} \nu_2 + 2 \sqrt{\frac{y_1}{y_2 z_1}} \nu_3 - \sqrt{\frac{y_1}{y_2 z_1}} - \sqrt{\frac{y_2}{y_1 z_1}} \right) - 2 \sqrt{\frac{y_1 z_1}{y_2}} \right. \right. \\
& \left. \left. - 2 \sqrt{\frac{y_2 z_1}{y_1}} \right) + \sin(z_2) \left( \left( -2 \left( \sqrt{\frac{y_1 z_1}{y_2}} + \sqrt{\frac{y_2 z_1}{y_1}} \right) + 4 \sqrt{\frac{y_2 z_1}{y_1}} \nu_2 + 4 \sqrt{\frac{y_1 z_1}{y_2}} \nu_3 \right) z_2^2 \right. \right. \\
& \left. \left. - (2 \nu_3 - 1) \left( 2 \sqrt{\frac{y_2}{y_1 z_1}} \nu_2 + 2 \sqrt{\frac{y_1}{y_2 z_1}} \nu_3 - \sqrt{\frac{y_1}{y_2 z_1}} - \sqrt{\frac{y_2}{y_1 z_1}} \right) z_2 + 2 \left( -2 \sqrt{\frac{y_2 z_1}{y_1}} \nu_2 \right. \right. \right. \\
& \left. \left. \left. - 2 \sqrt{\frac{y_1 z_1}{y_2}} \nu_3 + \sqrt{\frac{y_1 z_1}{y_2}} + \sqrt{\frac{y_2 z_1}{y_1}} \right) \right) \right) - 2 H_{\nu_3}^{(1)}(y_2) H_{\nu_3}^{(2)}(z_1) \sin(z_2) \sqrt{\frac{y_1 z_1}{y_2}} \\
& \left. - 2 H_{\nu_3}^{(1)}(y_2) H_{\nu_3}^{(2)}(z_1) \sin(z_2) \sqrt{\frac{y_2 z_1}{y_1}} + 4 H_{\nu_3-1}^{(1)}(y_2) H_{\nu_3}^{(2)}(z_1) \sin(z_2) \sqrt{y_1 y_2 z_1} \right) \Big).
\end{aligned}$$

This expression remains quite complex, although it is much simpler compared to the original expression for  $\alpha_4 - \beta_4$ . We plot  $|\alpha_4 - \beta_4|^2 = |G_1|^2$  in Fig. 10(a). It can be observed that, in the limit where  $k \gg \bar{\mathcal{H}}_1$ , this approximation matches the numerical solution quite well.

To better match the numerical results across the entire frequency range, we propose a parameterized template as

$$\frac{P_T(k)}{P_{T,inf2}} = \frac{1}{1 + e^{k - \bar{\mathcal{H}}_3}} + |G_1|^2. \quad (\text{A15})$$

We compare this template with the numerical results in Fig. 10(b). It is evident that Eq.

(A15) serves as a reliable approximation for observational purposes.

---

- [1] S. L. Detweiler, “Pulsar timing measurements and the search for gravitational waves,” *Astrophys. J.* **234** (1979) 1100–1104.
- [2] **LIGO Scientific, Virgo** Collaboration, B. P. Abbott *et al.*, “Observation of Gravitational Waves from a Binary Black Hole Merger,” *Phys. Rev. Lett.* **116** no. 6, (2016) 061102, [arXiv:1602.03837 \[gr-qc\]](https://arxiv.org/abs/1602.03837).
- [3] **NANOGrav** Collaboration, G. Agazie *et al.*, “The NANOGrav 15 yr Data Set: Evidence for a Gravitational-wave Background,” *Astrophys. J. Lett.* **951** no. 1, (2023) L8, [arXiv:2306.16213 \[astro-ph.HE\]](https://arxiv.org/abs/2306.16213).
- [4] **NANOGrav** Collaboration, A. Afzal *et al.*, “The NANOGrav 15 yr Data Set: Search for Signals from New Physics,” *Astrophys. J. Lett.* **951** no. 1, (2023) L11, [arXiv:2306.16219 \[astro-ph.HE\]](https://arxiv.org/abs/2306.16219).
- [5] **NANOGrav** Collaboration, Z. Arzoumanian *et al.*, “The NANOGrav 12.5 yr Data Set: Search for an Isotropic Stochastic Gravitational-wave Background,” *Astrophys. J. Lett.* **905** no. 2, (2020) L34, [arXiv:2009.04496 \[astro-ph.HE\]](https://arxiv.org/abs/2009.04496).
- [6] **EPTA, InPTA**: Collaboration, J. Antoniadis *et al.*, “The second data release from the European Pulsar Timing Array - III. Search for gravitational wave signals,” *Astron. Astrophys.* **678** (2023) A50, [arXiv:2306.16214 \[astro-ph.HE\]](https://arxiv.org/abs/2306.16214).
- [7] D. J. Reardon *et al.*, “Search for an Isotropic Gravitational-wave Background with the Parkes Pulsar Timing Array,” *Astrophys. J. Lett.* **951** no. 1, (2023) L6, [arXiv:2306.16215 \[astro-ph.HE\]](https://arxiv.org/abs/2306.16215).
- [8] H. Xu *et al.*, “Searching for the Nano-Hertz Stochastic Gravitational Wave Background with the Chinese Pulsar Timing Array Data Release I,” *Res. Astron. Astrophys.* **23** no. 7, (2023) 075024, [arXiv:2306.16216 \[astro-ph.HE\]](https://arxiv.org/abs/2306.16216).
- [9] L. P. Grishchuk, “Amplification of gravitational waves in an isotropic universe,” *Zh. Eksp. Teor. Fiz.* **67** (1974) 825–838.
- [10] A. A. Starobinsky, “Spectrum of relict gravitational radiation and the early state of the universe,” *JETP Lett.* **30** (1979) 682–685.
- [11] V. A. Rubakov, M. V. Sazhin, and A. V. Veryaskin, “Graviton Creation in the Inflationary

- Universe and the Grand Unification Scale,” *Phys. Lett. B* **115** (1982) 189–192.
- [12] A. H. Guth, “The Inflationary Universe: A Possible Solution to the Horizon and Flatness Problems,” *Phys. Rev. D* **23** (1981) 347–356.
- [13] A. D. Linde, “A New Inflationary Universe Scenario: A Possible Solution of the Horizon, Flatness, Homogeneity, Isotropy and Primordial Monopole Problems,” *Phys. Lett. B* **108** (1982) 389–393.
- [14] A. Albrecht and P. J. Steinhardt, “Cosmology for Grand Unified Theories with Radiatively Induced Symmetry Breaking,” *Phys. Rev. Lett.* **48** (1982) 1220–1223.
- [15] A. A. Starobinsky, “A New Type of Isotropic Cosmological Models Without Singularity,” *Phys. Lett. B* **91** (1980) 99–102.
- [16] S. Vagnozzi, “Inflationary interpretation of the stochastic gravitational wave background signal detected by pulsar timing array experiments,” *JHEAp* **39** (2023) 81–98, [arXiv:2306.16912 \[astro-ph.CO\]](https://arxiv.org/abs/2306.16912).
- [17] J.-Q. Jiang, Y. Cai, G. Ye, and Y.-S. Piao, “Broken blue-tilted inflationary gravitational waves: a joint analysis of NANOGrav 15-year and BICEP/Keck 2018 data,” [arXiv:2307.15547 \[astro-ph.CO\]](https://arxiv.org/abs/2307.15547).
- [18] M. Zhu, G. Ye, and Y. Cai, “Pulsar timing array observations as possible hints for nonsingular cosmology,” *Eur. Phys. J. C* **83** no. 9, (2023) 816, [arXiv:2307.16211 \[astro-ph.CO\]](https://arxiv.org/abs/2307.16211).
- [19] G. Ye, M. Zhu, and Y. Cai, “Null energy condition violation during inflation and pulsar timing array observations,” *JHEP* **02** (2024) 008, [arXiv:2312.10685 \[gr-qc\]](https://arxiv.org/abs/2312.10685).
- [20] L. Frosina and A. Urbano, “Inflationary interpretation of the nHz gravitational-wave background,” *Phys. Rev. D* **108** no. 10, (2023) 103544, [arXiv:2308.06915 \[astro-ph.CO\]](https://arxiv.org/abs/2308.06915).
- [21] J. Ellis, M. Fairbairn, G. Franciolini, G. Hütsi, A. Iovino, M. Lewicki, M. Raidal, J. Urrutia, V. Vaskonen, and H. Veermäe, “What is the source of the PTA GW signal?,” *Phys. Rev. D* **109** no. 2, (2024) 023522, [arXiv:2308.08546 \[astro-ph.CO\]](https://arxiv.org/abs/2308.08546).
- [22] H.-L. Huang, Y. Cai, J.-Q. Jiang, J. Zhang, and Y.-S. Piao, “Supermassive primordial black holes in multiverse: for nano-Hertz gravitational wave and high-redshift JWST galaxies,” [arXiv:2306.17577 \[gr-qc\]](https://arxiv.org/abs/2306.17577).
- [23] X. K. Du, M. X. Huang, F. Wang, and Y. K. Zhang, “Did the nHZ Gravitational Waves Signatures Observed By NANOGrav Indicate Multiple Sector SUSY Breaking?,”

[arXiv:2307.02938 \[hep-ph\]](https://arxiv.org/abs/2307.02938).

- [24] Y.-M. Wu, Z.-C. Chen, and Q.-G. Huang, “Cosmological Interpretation for the Stochastic Signal in Pulsar Timing Arrays,” [arXiv:2307.03141 \[astro-ph.CO\]](https://arxiv.org/abs/2307.03141).
- [25] Y. Xiao, J. M. Yang, and Y. Zhang, “Implications of nano-Hertz gravitational waves on electroweak phase transition in the singlet dark matter model,” *Sci. Bull.* **68** (2023) 3158–3164, [arXiv:2307.01072 \[hep-ph\]](https://arxiv.org/abs/2307.01072).
- [26] C. Zhang, N. Dai, Q. Gao, Y. Gong, T. Jiang, and X. Lu, “Detecting new fundamental fields with pulsar timing arrays,” *Phys. Rev. D* **108** no. 10, (2023) 104069, [arXiv:2307.01093 \[gr-qc\]](https://arxiv.org/abs/2307.01093).
- [27] G. Ye and A. Silvestri, “Can the Gravitational Wave Background Feel Wiggles in Spacetime?,” *Astrophys. J. Lett.* **963** no. 1, (2024) L15, [arXiv:2307.05455 \[astro-ph.CO\]](https://arxiv.org/abs/2307.05455).
- [28] S. F. King, R. Roshan, X. Wang, G. White, and M. Yamazaki, “Quantum gravity effects on dark matter and gravitational waves,” *Phys. Rev. D* **109** no. 2, (2024) 024057, [arXiv:2308.03724 \[hep-ph\]](https://arxiv.org/abs/2308.03724).
- [29] M. X. Huang, F. Wang, and Y. K. Zhang, “The Interplay Between the Muon  $g - 2$  Anomaly and the PTA nHZ Gravitational Waves from Domain Walls in NMSSM,” [arXiv:2309.06378 \[hep-ph\]](https://arxiv.org/abs/2309.06378).
- [30] K. D. Lozanov, S. Pi, M. Sasaki, V. Takhistov, and A. Wang, “Axion Universal Gravitational Wave Interpretation of Pulsar Timing Array Data,” [arXiv:2310.03594 \[astro-ph.CO\]](https://arxiv.org/abs/2310.03594).
- [31] R. Maji and W.-I. Park, “Supersymmetric U(1)B-L flat direction and NANOGrav 15 year data,” *JCAP* **01** (2024) 015, [arXiv:2308.11439 \[hep-ph\]](https://arxiv.org/abs/2308.11439).
- [32] M. Kawasaki and K. Murai, “Enhancement of gravitational waves at Q-ball decay including non-linear density perturbations,” *JCAP* **01** (2024) 050, [arXiv:2308.13134 \[astro-ph.CO\]](https://arxiv.org/abs/2308.13134).
- [33] S. He, L. Li, S. Wang, and S.-J. Wang, “Constraints on holographic QCD phase transitions from PTA observations,” [arXiv:2308.07257 \[hep-ph\]](https://arxiv.org/abs/2308.07257).
- [34] S. Choudhury, K. Dey, A. Karde, S. Panda, and M. Sami, “Primordial non-Gaussianity as a saviour for PBH overproduction in SIGWs generated by Pulsar Timing Arrays for Galileon inflation,” [arXiv:2310.11034 \[astro-ph.CO\]](https://arxiv.org/abs/2310.11034).

- [35] S. Choudhury, K. Dey, and A. Karde, “Untangling PBH overproduction in  $w$ -SIGWs generated by Pulsar Timing Arrays for MST-EFT of single field inflation,” [arXiv:2311.15065 \[astro-ph.CO\]](https://arxiv.org/abs/2311.15065).
- [36] J.-Q. Jiang and Y.-S. Piao, “Search for the non-linearities of gravitational wave background in NANOGrav 15-year data set,” [arXiv:2401.16950 \[gr-qc\]](https://arxiv.org/abs/2401.16950).
- [37] M. De Angelis, A. Smith, W. Giarè, and C. van de Bruck, “Gravitational waves in a cyclic Universe: resilience through cycles and vacuum state,” [arXiv:2403.00533 \[hep-th\]](https://arxiv.org/abs/2403.00533).
- [38] **BICEP, Keck** Collaboration, P. A. R. Ade *et al.*, “Improved Constraints on Primordial Gravitational Waves using Planck, WMAP, and BICEP/Keck Observations through the 2018 Observing Season,” *Phys. Rev. Lett.* **127** no. 15, (2021) 151301, [arXiv:2110.00483 \[astro-ph.CO\]](https://arxiv.org/abs/2110.00483).
- [39] D. Borah, S. Jyoti Das, and R. Samanta, “Imprint of inflationary gravitational waves and WIMP dark matter in pulsar timing array data,” [arXiv:2307.00537 \[hep-ph\]](https://arxiv.org/abs/2307.00537).
- [40] S. Choudhury, “Single field inflation in the light of Pulsar Timing Array Data: Quintessential interpretation of blue tilted tensor spectrum through Non-Bunch Davies initial condition,” [arXiv:2307.03249 \[astro-ph.CO\]](https://arxiv.org/abs/2307.03249).
- [41] I. Ben-Dayan, U. Kumar, U. Thattarampilly, and A. Verma, “Probing the early Universe cosmology with NANOGrav: Possibilities and limitations,” *Phys. Rev. D* **108** no. 10, (2023) 103507, [arXiv:2307.15123 \[astro-ph.CO\]](https://arxiv.org/abs/2307.15123).
- [42] V. K. Oikonomou, “Flat energy spectrum of primordial gravitational waves versus peaks and the NANOGrav 2023 observation,” *Phys. Rev. D* **108** no. 4, (2023) 043516, [arXiv:2306.17351 \[astro-ph.CO\]](https://arxiv.org/abs/2306.17351).
- [43] S. Datta, “Explaining PTA Data with Inflationary GWs in a PBH-Dominated Universe,” [arXiv:2309.14238 \[hep-ph\]](https://arxiv.org/abs/2309.14238).
- [44] Y.-S. Piao and Y.-Z. Zhang, “Phantom inflation and primordial perturbation spectrum,” *Phys. Rev. D* **70** (2004) 063513, [arXiv:astro-ph/0401231](https://arxiv.org/abs/astro-ph/0401231).
- [45] M. Baldi, F. Finelli, and S. Matarrese, “Inflation with violation of the null energy condition,” *Phys. Rev. D* **72** (2005) 083504, [arXiv:astro-ph/0505552](https://arxiv.org/abs/astro-ph/0505552).
- [46] Y.-S. Piao, “Gravitational wave background from phantom superinflation,” *Phys. Rev. D* **73** (2006) 047302, [arXiv:gr-qc/0601115](https://arxiv.org/abs/gr-qc/0601115).
- [47] T. Kobayashi, M. Yamaguchi, and J. Yokoyama, “G-inflation: Inflation driven by the

- Galileon field,” *Phys. Rev. Lett.* **105** (2010) 231302, [arXiv:1008.0603 \[hep-th\]](#).
- [48] T. Kobayashi, M. Yamaguchi, and J. Yokoyama, “Generalized G-inflation: Inflation with the most general second-order field equations,” *Prog. Theor. Phys.* **126** (2011) 511–529, [arXiv:1105.5723 \[hep-th\]](#).
- [49] S. Endlich, A. Nicolis, and J. Wang, “Solid Inflation,” *JCAP* **10** (2013) 011, [arXiv:1210.0569 \[hep-th\]](#).
- [50] Y.-F. Cai, J.-O. Gong, S. Pi, E. N. Saridakis, and S.-Y. Wu, “On the possibility of blue tensor spectrum within single field inflation,” *Nucl. Phys. B* **900** (2015) 517–532, [arXiv:1412.7241 \[hep-th\]](#).
- [51] J.-O. Gong, “Blue running of the primordial tensor spectrum,” *JCAP* **07** (2014) 022, [arXiv:1403.5163 \[astro-ph.CO\]](#).
- [52] D. Cannone, G. Tasinato, and D. Wands, “Generalised tensor fluctuations and inflation,” *JCAP* **01** (2015) 029, [arXiv:1409.6568 \[astro-ph.CO\]](#).
- [53] Y. Wang and W. Xue, “Inflation and Alternatives with Blue Tensor Spectra,” *JCAP* **10** (2014) 075, [arXiv:1403.5817 \[astro-ph.CO\]](#).
- [54] S. Kuroyanagi, T. Takahashi, and S. Yokoyama, “Blue-tilted Tensor Spectrum and Thermal History of the Universe,” *JCAP* **02** (2015) 003, [arXiv:1407.4785 \[astro-ph.CO\]](#).
- [55] Y. Cai, Y.-T. Wang, and Y.-S. Piao, “Is there an effect of a nontrivial  $c_T$  during inflation?,” *Phys. Rev. D* **93** no. 6, (2016) 063005, [arXiv:1510.08716 \[astro-ph.CO\]](#).
- [56] Y. Cai, Y.-T. Wang, and Y.-S. Piao, “Propagating speed of primordial gravitational waves and inflation,” *Phys. Rev. D* **94** no. 4, (2016) 043002, [arXiv:1602.05431 \[astro-ph.CO\]](#).
- [57] Y.-T. Wang, Y. Cai, Z.-G. Liu, and Y.-S. Piao, “Probing the primordial universe with gravitational waves detectors,” *JCAP* **01** (2017) 010, [arXiv:1612.05088 \[astro-ph.CO\]](#).
- [58] T. Fujita, S. Kuroyanagi, S. Mizuno, and S. Mukohyama, “Blue-tilted Primordial Gravitational Waves from Massive Gravity,” *Phys. Lett. B* **789** (2019) 215–219, [arXiv:1808.02381 \[gr-qc\]](#).
- [59] S. Kuroyanagi, T. Takahashi, and S. Yokoyama, “Blue-tilted inflationary tensor spectrum and reheating in the light of NANOGrav results,” *JCAP* **01** (2021) 071, [arXiv:2011.03323 \[astro-ph.CO\]](#).
- [60] S. Akama, S. Hirano, and T. Kobayashi, “Primordial tensor non-Gaussianities from general single-field inflation with non-Bunch-Davies initial states,” *Phys. Rev. D* **102** no. 2, (2020)

023513, [arXiv:2003.10686 \[gr-qc\]](#).

- [61] S. Akama and H. W. H. Tahara, “Imprints of primordial gravitational waves with non-Bunch-Davies initial states on CMB bispectra,” *Phys. Rev. D* **108** no. 10, (2023) 103522, [arXiv:2306.17752 \[gr-qc\]](#).
- [62] W. Giarè, F. Renzi, and A. Melchiorri, “Higher-Curvature Corrections and Tensor Modes,” *Phys. Rev. D* **103** no. 4, (2021) 043515, [arXiv:2012.00527 \[astro-ph.CO\]](#).
- [63] W. Giarè, M. Forconi, E. Di Valentino, and A. Melchiorri, “Towards a reliable calculation of relic radiation from primordial gravitational waves,” *Mon. Not. Roy. Astron. Soc.* **520** (2023) 2, [arXiv:2210.14159 \[astro-ph.CO\]](#).
- [64] V. K. Oikonomou, “A Stiff Pre-CMB Era with a Mildly Blue-tilted Tensor Inflationary Era can Explain the 2023 NANOGrav Signal,” [arXiv:2309.04850 \[astro-ph.CO\]](#).
- [65] V. K. Oikonomou, P. Tsyba, and O. Razina, “Red or blue tensor spectrum from GW170817-compatible Einstein-Gauss-Bonnet theory: A detailed analysis,” *EPL* **145** no. 4, (2024) 49001, [arXiv:2402.02049 \[gr-qc\]](#).
- [66] V. Rubakov, “The Null Energy Condition and its violation,” *Usp. Fiz. Nauk* **184** no. 2, (2014) 137–152, [arXiv:1401.4024 \[hep-th\]](#).
- [67] M. Libanov, S. Mironov, and V. Rubakov, “Generalized Galileons: instabilities of bouncing and Genesis cosmologies and modified Genesis,” *JCAP* **08** (2016) 037, [arXiv:1605.05992 \[hep-th\]](#).
- [68] T. Kobayashi, “Generic instabilities of nonsingular cosmologies in Horndeski theory: A no-go theorem,” *Phys. Rev. D* **94** no. 4, (2016) 043511, [arXiv:1606.05831 \[hep-th\]](#).
- [69] D. A. Easson, I. Sawicki, and A. Vikman, “G-Bounce,” *JCAP* **11** (2011) 021, [arXiv:1109.1047 \[hep-th\]](#).
- [70] T. Qiu and Y.-T. Wang, “G-Bounce Inflation: Towards Nonsingular Inflation Cosmology with Galileon Field,” *JHEP* **04** (2015) 130, [arXiv:1501.03568 \[astro-ph.CO\]](#).
- [71] A. Ijjas and P. J. Steinhardt, “Classically stable nonsingular cosmological bounces,” *Phys. Rev. Lett.* **117** no. 12, (2016) 121304, [arXiv:1606.08880 \[gr-qc\]](#).
- [72] A. Ijjas and P. J. Steinhardt, “Fully stable cosmological solutions with a non-singular classical bounce,” *Phys. Lett. B* **764** (2017) 289–294, [arXiv:1609.01253 \[gr-qc\]](#).
- [73] D. A. Dobre, A. V. Frolov, J. T. Gálvez Ghersi, S. Ramazanov, and A. Vikman, “Unbraiding the Bounce: Superluminality around the Corner,” *JCAP* **03** (2018) 020,

[arXiv:1712.10272 \[gr-qc\]](https://arxiv.org/abs/1712.10272).

- [74] Y. Cai, Y. Wan, H.-G. Li, T. Qiu, and Y.-S. Piao, “The Effective Field Theory of nonsingular cosmology,” *JHEP* **01** (2017) 090, [arXiv:1610.03400 \[gr-qc\]](https://arxiv.org/abs/1610.03400).
- [75] P. Creminelli, D. Pirtskhalava, L. Santoni, and E. Trincherini, “Stability of Geodesically Complete Cosmologies,” *JCAP* **11** (2016) 047, [arXiv:1610.04207 \[hep-th\]](https://arxiv.org/abs/1610.04207).
- [76] Y. Cai, H.-G. Li, T. Qiu, and Y.-S. Piao, “The Effective Field Theory of nonsingular cosmology: II,” *Eur. Phys. J. C* **77** no. 6, (2017) 369, [arXiv:1701.04330 \[gr-qc\]](https://arxiv.org/abs/1701.04330).
- [77] Y. Cai and Y.-S. Piao, “A covariant Lagrangian for stable nonsingular bounce,” *JHEP* **09** (2017) 027, [arXiv:1705.03401 \[gr-qc\]](https://arxiv.org/abs/1705.03401).
- [78] R. Kolevatov, S. Mironov, N. Sukhov, and V. Volkova, “Cosmological bounce and Genesis beyond Horndeski,” *JCAP* **08** (2017) 038, [arXiv:1705.06626 \[hep-th\]](https://arxiv.org/abs/1705.06626).
- [79] Y. Cai and Y.-S. Piao, “Higher order derivative coupling to gravity and its cosmological implications,” *Phys. Rev. D* **96** no. 12, (2017) 124028, [arXiv:1707.01017 \[gr-qc\]](https://arxiv.org/abs/1707.01017).
- [80] Y. Cai, Y.-T. Wang, J.-Y. Zhao, and Y.-S. Piao, “Primordial perturbations with pre-inflationary bounce,” *Phys. Rev. D* **97** no. 10, (2018) 103535, [arXiv:1709.07464 \[astro-ph.CO\]](https://arxiv.org/abs/1709.07464).
- [81] S. Mironov, V. Rubakov, and V. Volkova, “Bounce beyond Horndeski with GR asymptotics and  $\gamma$ -crossing,” *JCAP* **10** (2018) 050, [arXiv:1807.08361 \[hep-th\]](https://arxiv.org/abs/1807.08361).
- [82] T. Qiu, K. Tian, and S. Bu, “Perturbations of bounce inflation scenario from  $f(T)$  modified gravity revisited,” *Eur. Phys. J. C* **79** no. 3, (2019) 261, [arXiv:1810.04436 \[gr-qc\]](https://arxiv.org/abs/1810.04436).
- [83] G. Ye and Y.-S. Piao, “Implication of GW170817 for cosmological bounces,” *Commun. Theor. Phys.* **71** no. 4, (2019) 427, [arXiv:1901.02202 \[gr-qc\]](https://arxiv.org/abs/1901.02202).
- [84] G. Ye and Y.-S. Piao, “Bounce in general relativity and higher-order derivative operators,” *Phys. Rev. D* **99** no. 8, (2019) 084019, [arXiv:1901.08283 \[gr-qc\]](https://arxiv.org/abs/1901.08283).
- [85] S. Mironov, V. Rubakov, and V. Volkova, “Genesis with general relativity asymptotics in beyond Horndeski theory,” *Phys. Rev. D* **100** no. 8, (2019) 083521, [arXiv:1905.06249 \[hep-th\]](https://arxiv.org/abs/1905.06249).
- [86] S. Akama, S. Hirano, and T. Kobayashi, “Primordial non-Gaussianities of scalar and tensor perturbations in general bounce cosmology: Evading the no-go theorem,” *Phys. Rev. D* **101** no. 4, (2020) 043529, [arXiv:1908.10663 \[gr-qc\]](https://arxiv.org/abs/1908.10663).
- [87] S. Mironov, V. Rubakov, and V. Volkova, “Subluminal cosmological bounce beyond

- Horndeski,” *JCAP* **05** (2020) 024, [arXiv:1910.07019 \[hep-th\]](#).
- [88] A. Ilyas, M. Zhu, Y. Zheng, Y.-F. Cai, and E. N. Saridakis, “DHOST Bounce,” *JCAP* **09** (2020) 002, [arXiv:2002.08269 \[gr-qc\]](#).
- [89] A. Ilyas, M. Zhu, Y. Zheng, and Y.-F. Cai, “Emergent Universe and Genesis from the DHOST Cosmology,” *JHEP* **01** (2021) 141, [arXiv:2009.10351 \[gr-qc\]](#).
- [90] M. Zhu, A. Ilyas, Y. Zheng, Y.-F. Cai, and E. N. Saridakis, “Scalar and tensor perturbations in DHOST bounce cosmology,” *JCAP* **11** no. 11, (2021) 045, [arXiv:2108.01339 \[gr-qc\]](#).
- [91] M. Zhu and Y. Zheng, “Improved DHOST Genesis,” *JHEP* **11** (2021) 163, [arXiv:2109.05277 \[gr-qc\]](#).
- [92] S. Mironov and V. Volkova, “Stable nonsingular cosmologies in beyond Horndeski theory and disformal transformations,” *Int. J. Mod. Phys. A* **37** no. 14, (2022) 2250088, [arXiv:2204.05889 \[hep-th\]](#).
- [93] Y. Cai, J. Xu, S. Zhao, and S. Zhou, “Perturbative unitarity and NEC violation in genesis cosmology,” *JHEP* **10** (2022) 140, [arXiv:2207.11772 \[gr-qc\]](#). [Erratum: JHEP 11, 063 (2022)].
- [94] A. Panda, D. Gangopadhyay, and G. Manna, “NEC violation in  $f(\bar{R}, \bar{T})$  gravity in the context of a non-canonical theory via modified Raychaudhuri equation,” [arXiv:2402.18431 \[gr-qc\]](#).
- [95] Y. Cai and Y.-S. Piao, “Intermittent null energy condition violations during inflation and primordial gravitational waves,” *Phys. Rev. D* **103** no. 8, (2021) 083521, [arXiv:2012.11304 \[gr-qc\]](#).
- [96] Y. Cai and Y.-S. Piao, “Generating enhanced primordial GWs during inflation with intermittent violation of NEC and diminishment of GW propagating speed,” *JHEP* **06** (2022) 067, [arXiv:2201.04552 \[gr-qc\]](#).
- [97] Z.-C. Chen and L. Liu, “Constraints on Null Energy Condition Violation from Advanced LIGO and Advanced Virgo’s First Three Observing Runs,” [arXiv:2404.07075 \[gr-qc\]](#).
- [98] Z.-C. Chen and L. Liu, “Detecting a Gravitational-Wave Background from Null Energy Condition Violation: Prospects for Taiji,” [arXiv:2404.08375 \[gr-qc\]](#).
- [99] Y. Cai, M. Zhu, and Y.-S. Piao, “Primordial black holes from null energy condition violation during inflation,” [arXiv:2305.10933 \[gr-qc\]](#).

- [100] Y. Cai, “Generating enhanced parity-violating gravitational waves during inflation with violation of the null energy condition,” *Phys. Rev. D* **107** no. 6, (2023) 063512, [arXiv:2212.10893 \[gr-qc\]](https://arxiv.org/abs/2212.10893).
- [101] M. Zhu and Y. Cai, “Parity-violation in bouncing cosmology,” *JHEP* **04** (2023) 095, [arXiv:2301.13502 \[gr-qc\]](https://arxiv.org/abs/2301.13502).
- [102] Y. Cai, Y.-T. Wang, and Y.-S. Piao, “Preinflationary primordial perturbations,” *Phys. Rev. D* **92** no. 2, (2015) 023518, [arXiv:1501.01730 \[astro-ph.CO\]](https://arxiv.org/abs/1501.01730).
- [103] Y. Cai and Y.-S. Piao, “Pre-inflation and trans-Planckian censorship,” *Sci. China Phys. Mech. Astron.* **63** no. 11, (2020) 110411, [arXiv:1909.12719 \[gr-qc\]](https://arxiv.org/abs/1909.12719).
- [104] M. S. Turner, M. J. White, and J. E. Lidsey, “Tensor perturbations in inflationary models as a probe of cosmology,” *Phys. Rev. D* **48** (1993) 4613–4622, [arXiv:astro-ph/9306029](https://arxiv.org/abs/astro-ph/9306029).
- [105] L. A. Boyle and P. J. Steinhardt, “Probing the early universe with inflationary gravitational waves,” *Phys. Rev. D* **77** (2008) 063504, [arXiv:astro-ph/0512014](https://arxiv.org/abs/astro-ph/0512014).
- [106] W. Zhao and Y. Zhang, “Relic gravitational waves and their detection,” *Phys. Rev. D* **74** (2006) 043503, [arXiv:astro-ph/0604458](https://arxiv.org/abs/astro-ph/0604458).